

A Study on an Improved Technique to Determine Impact Location of Loose Part in Reactor Coolant System

Yong-Beum Kim, Hea-Dong Chung, Myung-Jo Jhung and Youn Won Park

Korea Institute of Nuclear Safety
Mechanical and Material Department
19 Kusung-dong, Yusung-gu, Taejeon, Korea, 305-600

Abstract

A loose part, located in the reactor coolant system (RCS) of a nuclear power plant (NPP), can cause damage to the components of the RCS by impacting on the components and can threaten the safety of the NPP. Therefore a reliable means to detect a loose part should be provided to secure the safety of the NPP. Detection of a loose part is accomplished using sensors attached to the components which measures the signals generated by the impacts of the loose part on the components

Through this study, an improved technique to determine the loose part location has been developed for the reactor coolant system of a nuclear power plant. The adoption of the Wigner-Ville distribution function makes it possible to reduce the errors involved in determining the arrival time difference of waves on structures, which enables a more accurate evaluation of the loose part location.

Experiments were carried out to prove the performance and applicability of the improved technique. The experimental results show that the proposed technique determines the loose part location more accurately than conventional methods.

1. Introduction

A part of a mechanical component in the RCS may be loosened from its original location by various mechanisms, such as fatigue damage due to flow-induced vibration. Since the loose part circulates with reactor coolants in the RCS, it may make repetitive contact with the components of the RCS. This may damage the structural integrity of the components, therefore it is necessary to identify the location of the loose part and to remove the loose part from the RCS in order to secure the safety of the NPP. Due to this necessity, much research has been carried out for the development of techniques to determine loose part location.

Krister⁽¹⁾ introduced a method to determine impact location using both the arrival time

difference and the damping value of impact signals measured with two accelerometers. Olma⁽²⁾ also introduced another method to determine the impact location using both the arrival time difference between longitudinal and transverse waves measured with one accelerometer and the propagation velocity of the two waves.

Since these methods use only the shape of time history of impact signals, the estimation of the arrival time difference depends on the sensitivity of the accelerometers and the noise level. Therefore, these methods have an obvious limitation on the estimation of the arrival time difference. When an impact is made on a plate, three kinds of waves are generated, longitudinal, transverse, and bending waves. Since the longitudinal and transverse waves are relatively smaller than bending waves, the signals measured with the sensors represent mainly characteristics of bending waves. Therefore, it is extremely difficult to extract the longitudinal and transverse waves from the impact signals practically. In order to overcome the deficiencies in the conventional methods, a new method using bending waves will be introduced in this paper.

This method uses dispersion characteristics of bending waves such as propagation velocity and arrival time difference of bending waves with different frequencies. The dispersion characteristics of bending waves can be obtained through the transformation of impact signals using the Wigner-Ville distribution function. The distance from the impact location to the signal measuring point can be calculated using information on propagation velocity and arrival time difference of two bending waves having different frequencies.

2. Wigner-Ville Distribution Function

When non-stationary signals like a transient signal are interpreted, signal analysis in frequency domain, a method mainly used in interpreting stationary signals, can handle only part of the signal information, and hence it has to be accompanied with signal analysis in time domain.

As one of the methods enabling simultaneous signal analysis in time and frequency domain, the Wigner-Ville distribution function is drawing a lot of attention lately. The Wigner-Ville distribution function was first proposed by Wigner in 1932, and concept of the function was re-established by Ville in 1948. The following is a definition of the Wigner-Ville distribution function which is expressed by consecutive time and frequency⁽³⁾.

$$W(t, \omega) = \int_{-}^{+} s\left(t + \frac{\tau}{2}\right) s^*\left(t - \frac{\tau}{2}\right) e^{-j\omega\tau} d\tau \quad (1)$$

Here, t , ω , and τ represent time, frequency and time delay respectively. $s(t)$ is time history, and the asterisk(*) denotes the complex conjugate. $W(t, \omega)$ means the Wigner-Ville distribution function, which is a function of time and frequency. According to the equation (1), the Wigner-Ville distribution function is Fourier transform value for the time delay τ of $s\left(t + \frac{\tau}{2}\right) s^*\left(t - \frac{\tau}{2}\right)$ which is a time-dependent autocorrelation function, and represents the

distribution of power on the time-frequency plane⁽⁴⁾.

Accordingly, the total energy of the signal can be obtained by integrating the Wigner-Ville distribution function for the entire time and frequency range. Also when we integrate the Wigner-Ville distribution function for a frequency range at a particular time t , we can obtain an instant signal power at that time. When we integrate the Wigner-Ville distribution function for a time range at a particular frequency ω , we can obtain the energy spectrum density at that frequency.

In order to calculate the Wigner-Ville distribution function from signal data of limited record length, we need calculate an approximate discrete value of the equation (1). The approximate discrete value of the equation (1) can be expressed as follows.

$$W(m \Delta t, n \Delta \omega) \approx 2 \Delta t \sum_{k=-N}^{N-1} g_m(k) e^{-i2\pi n k / K} \quad (2)$$

Here, $g_m(k) = s[(m+k)\Delta t]s^*[(m-k)\Delta t]$, where k, m and n are integers, N is the number of time history data. Also $K = 2N$, $\Delta\omega = \pi/K\Delta t$ and Δt is a sampling time. Using the periodicity of signal data with limited record length, we can express the equation (2) as follows⁽⁵⁾.

$$W(m \Delta t, n \Delta \omega) \approx 2 \Delta t \sum_{k=0}^{K-1} g_m(k) e^{-i2\pi n k / K} \quad (3)$$

We can see that $W(m \Delta t, n \Delta \omega)$ from equation (3) is related to the discrete Fourier transform(DFT) of $g_m(k)$. In view point of signal processing of discrete signals, calculation of the Wigner-Ville distribution function requires a different method of signal processing from the general signal processing method.

In order to obtain from equation (3) the Wigner-Ville distribution function for time history whose data number is N , the DFT for number of $2N$ must be carried out. Also in the equation(1), since $s(t + \frac{\tau}{2})s^*(t - \frac{\tau}{2})$ is a function of the product of $s(t)$ distanced by the integral variable $\frac{\tau}{2}$ on both sides of time t , the sampling frequency diminishes by one-half the sample frequency of the original signal $s(t)$ when analyzing the Wigner-Ville distribution function. As a result, in order to avoid the aliasing phenomenon when analyzing the Wigner-Ville distribution function, the Nyquist frequency must be limited to 1/4 of the sampling frequency of $s(t)$ signal. With respect to the Nyquist frequency, if we use the complex analytic signal obtained by the Hilbert transform instead of using the actual time signal, when calculating the Wigner-Ville distribution function, we can take the Nyquist frequency to 1/2 of the $s(t)$ signal sampling frequency.

In equation (2), when we consider that the frequency resolution range of the Wigner-Ville distribution function is $\Delta\omega = \pi/2N\Delta t$, and the frequency resolution range is $2\pi/N\Delta t$ when taking general signal processing for the identical signal, we can tell that the frequency

resolution range of the Wigner-Ville distribution function is 1/4 smaller than the frequency resolution range for general signal processing, and hence the frequency resolution range improves.

Another characteristics of the Wigner-Ville distribution function is that, since it is a bilinear transformation, the value of the function can be either positive or negative, and that interference may occur in the function. Interference occurs when there is a cross-correlation among signal components, and when interference occurs the value of the Wigner-Ville distribution function appears in a varied form, hence increasing distribution error.

One method of solving the problem of the Wigner-Ville distribution function having negative values, and minimizing the distribution error is to smooth the function. The smoothing method is done by carrying out a two-dimensional convolution integration of the Wigner-Ville distribution function and the smoothing function along the time and frequency axis. The smoothed Wigner-Ville distribution function is expressed as follows.

$$W_s(t, \omega) = \int_{-}^{+} W(t-t', \omega-\omega') G(t', \omega') dt' d\omega' \quad (4)$$

Here $W_s(t, \omega)$ represents the smoothed Wigner-Ville distribution function, $W(t, \omega)$ represents the function before it is smoothed, and $G(t, \omega)$ represents the smoothing function. In general, for a smoothing function, Gaussian window is frequently used, and its form is as follows.

$$G(t, \omega) = \frac{1}{2\pi\sigma_t\sigma_\omega} \exp\left[-\left(\frac{t^2}{2\sigma_t^2} + \frac{\omega^2}{2\sigma_\omega^2}\right)\right] \quad (5)$$

Here, σ_t, σ_ω represents the standard deviation for each time and frequency range, and it determines the size of the Gaussian window. Cartwright proved that the values of σ_t^2 and σ_ω^2 are all positive, and that the smoothed Wigner-Ville distribution function is always positive when $\sigma_t^2 \sigma_\omega^2 \geq 1/4$ ⁽⁷⁾. And it must be noted that, when the Wigner-Ville distribution function is smoothed, interference can be reduced, but the resolution range of the time and frequency can be increased.

One of the useful characteristics of the Wigner-Ville distribution function is that the primary momentum obtained along the time axis has the same value as the group delay for each frequency. The equation for the group delay $\tau(\omega)$ is as follows⁽⁶⁾.

$$\tau(\omega) = \frac{\int_{-}^{+} t W(t, \omega) dt}{\int_{-}^{+} W(t, \omega) dt} \quad (6)$$

The characteristics of the Wigner-Ville distribution function concerning group delay are used effectively for analysis of the characteristics of bending wave propagation in plates, in other words, it is used for calculating the arrival time of bending wave.

3. Dispersion Characteristics of Bending Waves in Flat Plate

When a wave manifold consisting of waves with different frequencies propagates in a media and each wave with different frequencies propagates at different velocities, we call this phenomena dispersion. Bending waves in a flat plate show dispersion characteristics when they are propagated on the surface of the flat plate. A high frequency bending wave having a short wave length propagates at a high velocity while a low frequency bending wave having a long wave length propagates at a low velocity.

The equation of bending wave propagation on a flat plate, showing dispersion characteristics, can be derived from the wave equation on a flat plate as follows:

$$C_B = \left(\frac{EI}{m}\right)^{\frac{1}{4}} (\omega)^{\frac{1}{2}} \quad (7)$$

Here, C_B is the propagation velocity of the bending wave, E is Young's modulus of a flat plate, I is the cross-sectional 2nd moment per unit area, m is the mass per unit area, and ω is the angular frequency. In equation (7), the propagating velocity of bending waves is proportional to the square root of the angular frequency and is the same as the phase velocity, that is the velocity of phase propagation. The group velocity of waves which represents energy propagation velocity, is defined as follows⁽⁷⁾:

$$C_g = \frac{d\omega}{dk} \quad (8)$$

Here, C_g is group velocity and k is the wave number. From equation (8) and the wave equation of bending waves representing the relationship between angular frequency and wave number, it is derived that the group velocity of bending waves on a flat plate is twice the phase velocity as follows⁽⁷⁾:

$$C_g = 2 C_B \quad (9)$$

4. Method for Estimating an Impact Location

Generally, if an impact is made at a point on a plate as shown in Fig. 1, then bending waves with various frequencies are generated and propagated in a radial direction simultaneously, but the arrival time of each bending wave at a measuring point on the plate is not the same due to the dispersion characteristics of bending waves. That is, at a measuring point, bending waves with high frequency arrive earlier than those with low frequency due to the difference of propagation velocity.

Therefore, if we can measure the time that each bending wave with various frequencies

proceeds to a certain distance, then it is possible to infer the propagation velocity of bending waves experimentally.

Generally, an acceleration signal obtained at an accelerometer displays manifold characteristics of bending waves with various frequencies. Using equation (1), the acceleration signal can be transformed into a Wigner-Ville power distribution, which represents the time dependent power distribution of each bending wave with various frequencies in a time and frequency domain as shown in Fig. 2. The Wigner-Ville power distribution of a bending wave with a certain frequency has several peaks. The first peak corresponds to the maximum power of the original bending wave without influence of reflected waves and the remaining peaks signify the maximum power of reflected waves. Therefore, the curve connecting the first peaks of the Wigner-Ville power distribution of signals (called "arrival time curve") represents the arrival time of bending waves with various frequencies at a measuring point. A typical example of the arrival time curve is shown in Fig. 3, which is derived from the Wigner-Ville power distribution of signals received at two points A and B. Here, we can easily find that the measuring point A is closer to the impact location than point B, since the arrival time curve at point A is closer to the axis of "t=0" than the curve at point B. From Fig. 3, we can estimate the time that a bending wave with a certain frequency proceeds to the distance from A to B ($r_B - r_A$). Therefore, if the distance of $r_B - r_A$ is known, it is possible to estimate the propagation velocity of a bending wave with a certain frequency using equation (10).

$$v_f = \frac{r_B - r_A}{\Delta t_f} \quad (10)$$

where, v_f is the propagation velocity of a bending wave with frequency f and Δt_f is the traveling time of a bending wave with frequency f by the distance of $r_B - r_A$.

If two propagation velocities of bending waves with frequencies f_1 and f_2 and the arrival time difference between the two bending waves at the point A are known, the distance r_A between the impact location and A can be estimated using equation (11).

$$r_A = \Delta t_{f_1, f_2} v_{f_1} v_{f_2} / (v_{f_1} - v_{f_2}) \quad (11)$$

where, $\Delta t_{f_1, f_2}$ is the arrival time difference between two bending waves with frequencies f_1 and f_2 , at point A, respectively, and v_{f_1}, v_{f_2} are propagation velocities of bending waves with frequencies f_1 and f_2 , respectively.

Similarly, the distance of r_B and r_C can be estimated. Finally, if we draw circles around the center points of A, B, and C with corresponding radiuses r_A , r_B , and r_C as shown in Fig. 1, we can see that the intersection point of the circles is the impact location of a loose part.

5. Experimental Results

Experiments were carried out to prove the performance and the applicability of the proposed method. The experimental setup is shown in Fig. 1. A plate is hung at its upper two supports. Accelerometers are mounted at points A, B, and C on the plate, and an impact is made at point O. The plate is of rectangular shape with width, length, and thickness of 1.5 m, 1.2 m, and 5 mm, respectively, and the material is steel with a density and Young's modulus (E) of $7,860\text{kg/m}^3$ and 200GPa , respectively. The theoretical propagation velocity of bending waves of this plate is expressed as equation (12) from equation (7).

$$C_B = \left(\frac{EI}{m}\right)^{\frac{1}{4}} (\omega)^{\frac{1}{2}} = 6.925\sqrt{f} \quad (m/s) \quad (12)$$

where f represents frequency of bending waves.

Positions of the accelerometers (B&K Type 4393) and their distances from the origin O on the plate are given in table 1.

Table 1 Position and distance of accelerometers

	x (cm)	y (cm)	r (cm)
A	0	- 40	40
B	40	30	50
C	- 50	40	64

An impact signal is generated by an impact hammer (B&K Type #8202) and the impact location is determined to be the geometric center of the plate in order to minimize the reflection effect of bending waves from the edge of the plate. Signals received by impact hammer and accelerometers are amplified by a four channel pre-amplifier (B&K Type NEXUS) and acquired by an analyzer (B&K Type PULSE 3560) with a sampling rate of 65kHz.

The time history of the signals measured at the impact hammer and three accelerometers are shown in Fig. 4. From Fig. 4, we can confirm that the bending waves arrive earlier at the accelerometer located closer to the impact position while the reflected bending waves arrive earlier at the accelerometers located closer to the edge of the plate. Due to dispersion characteristics, the bending wave with a high frequency arrives earlier at the accelerometer.

Contour lines of the Wigner-Ville power distribution in time-frequency plane for acceleration signal at point A are shown in Fig. 5. The first contour line (closest to the axis of "t=0") represents the arrival time of bending waves with various frequencies at point A, the center line of which corresponds to the arrival time curve. The remaining contour lines signify the arrival time of reflected bending waves at point A. Here, we can notice that the first contour line is not parallel to the frequency-axis due to the dispersion characteristics of bending waves. Similarly, the arrival time curves can be obtained at points B and C.

Fig. 6 presents the arrival time curves at points A, B, and C, which corresponds to the arrival time of bending waves at points A, B, and C.

Fig.7 indicates power velocity vs. frequency of bending waves, which was determined from equation (10) using both the distances from the impact location to two accelerometers and the arrival time difference of bending waves determined from Fig. 6. The propagation velocity for each frequency determined using the experimental results shows that the relative percentage error is about 10% compared with the theoretical velocity determined from equation (7).

Fig. 8 shows histograms of r_c , which is the distance from the impact location to point C. They are calculated from equation (11) using two arbitrary velocities of bending waves in the frequency range of 1000 ~ 2000 Hz and the arrival time difference of the two bending waves at point C. In Fig. 8, the median value is estimated to be the r_c . Fig. 8(a) and Fig. 8(b) show r_c 's estimated value using the theoretical and experimental velocity information, respectively. Comparing these two results, the deviation of the experimental result from the true value is smaller than the theoretical one. This seems to arise from the fact that material properties of the plate used in the calculation of equation (12) may be different from the actual value. Similarly, r_A and r_B can be obtained using the experimental results. In table 2, the estimated r_A , r_B , and r_c values are shown and the accuracy of the estimated results are within 10%.

Table 2 Estimation of impact position

	r_A	r_B	r_c
True (m)	0.4	0.5	0.64
Estimation (m)	0.43	0.52	0.63
Error (%)	7.5	4	1.5

6. Conclusion

A improved method to determine a loose part location is proposed, which may be applied to reactor coolant system of nuclear power plant. This method uses the Wigner-Ville distribution function in order to estimate the arrival time difference of bending waves with various frequencies.

Experiments were carried out to prove the performance and the applicability of the proposed method. The experimental results show that the propagation velocity of bending waves with various frequencies can be calculated using the arrival time difference between two measurement points.

Also, the distance between a measurement point and impact location of a loose part can be estimated using propagation velocity and arrival time difference between two bending waves with different frequencies at one measurement point. Experimental results for estimation of the distance shows relative percentage error to be within 10% compared with actual distance.

References

- (1) R. C. Krister and F. Shahrokhi, "Summary of Studies on Methods for Detecting, Locating, and Characterizing Metallic Loose Parts in Nuclear Reactor Coolant System", *NUREG/CR-2344*, Washington D.C., Oct. 1981.
- (2) B. J. Olma, "Source Location and Mass Estimation in Loose Parts Monitoring of PWRs", *Progress in Nuclear Energy*, Vol. 15, pp. 583-594, Pergamon Press, 1985.
- (3) E. Wigner, "On the Quantum Correction for Thermodynamic Equilibrium," *Physical Review*, 40, pp. 749-759, 1932.
- (4) Y.-H. Kim and Y.-K. Park, "Wigner-Ville Interpretation of Musical Sound and Transient Vibration Signals," *WESTPRAC 1994*, pp.752-757, 1994.
- (5) T. J. Wahl and J. S. Bolton, "The Application of the Wigner Distribution to the Identification of Structure-Borne Noise Components," *J. Sound and Vibration*, 163(1), pp.101-122, 1993.
- (6) T.A.C.M. Claasen and W.F.G. Mecklenbrauker, "The Wigner Distribution - A Tool for Time-Frequency Signal Analysis; PART I : Continuous-Time Signals," *Philips J. Res.*, 35, pp.217-250, 1980.
- (7) L. Cremer, M. Heckl, "Structure-Borne Sound", *Springer-Verlag Berlin*, pp95-115, 1972

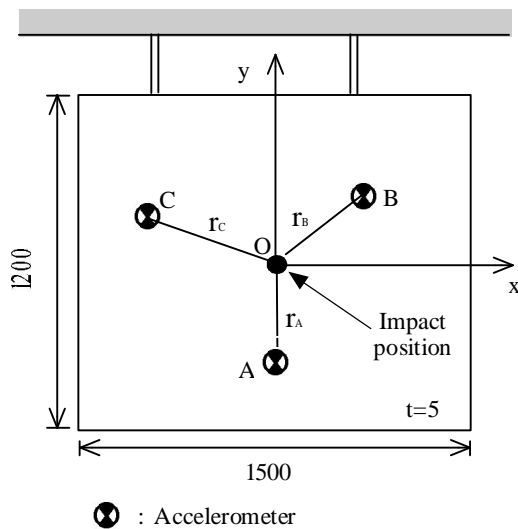


Fig. 1 Experimental setup

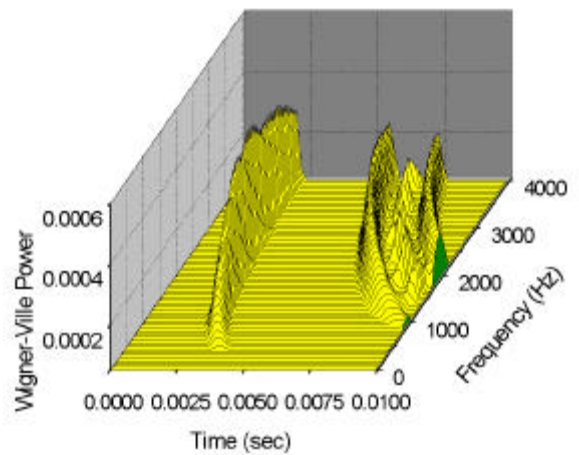


Fig. 2 Typical Wigner-Ville power distribution of impact signals measured with accelerometer

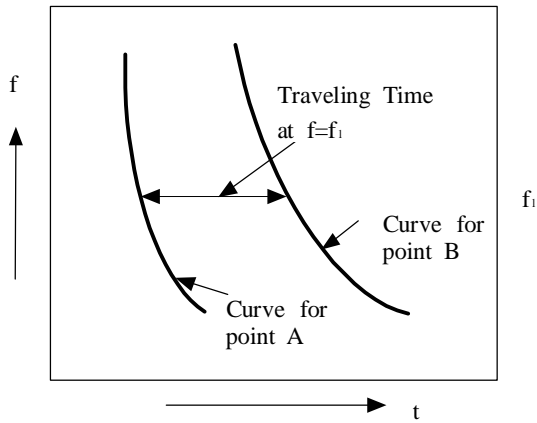


Fig. 3 An Illustration of arrival time curves

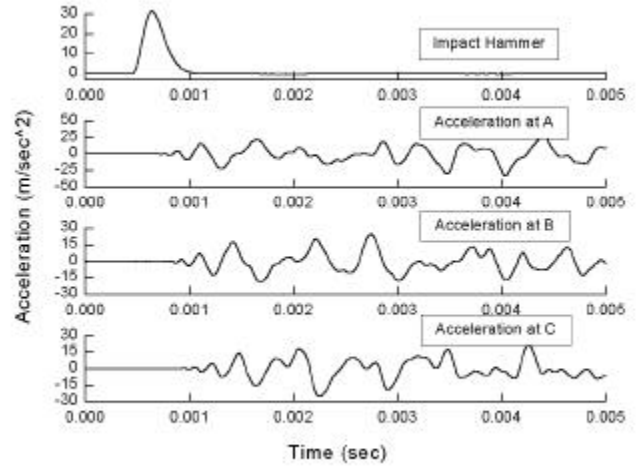


Fig. 4 Acceleration signals measured at impact hammer and 3 measuring points

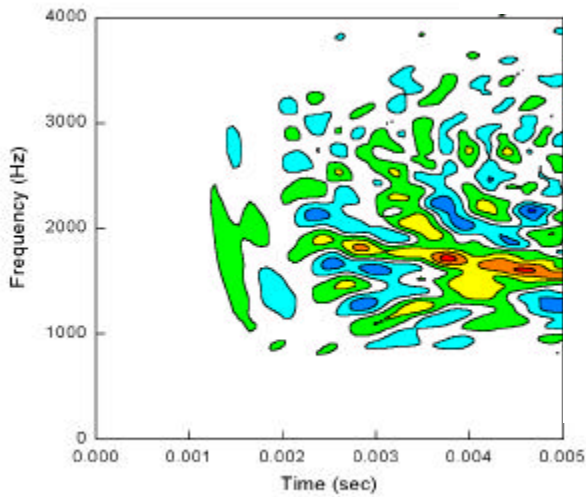


Fig. 5 Contour lines of Wigner-Ville power distribution at point A

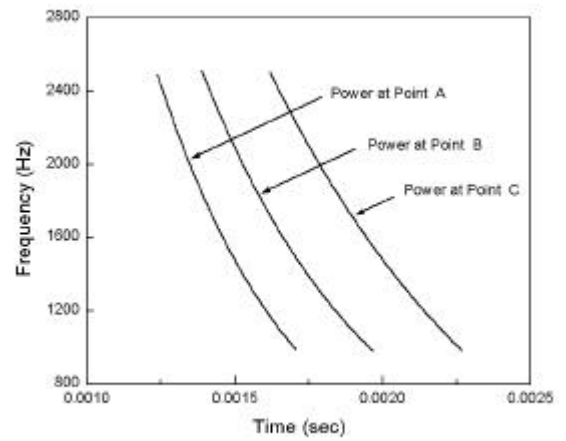


Fig. 6 Arrival time curves at the point A, B and C

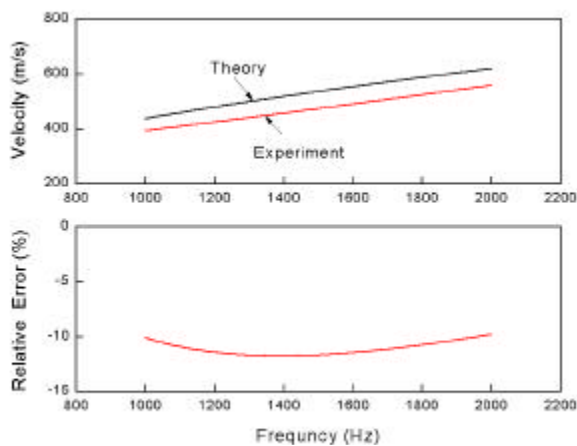


Fig. 7 Power velocity vs. frequency of bending waves and their relative percentage errors

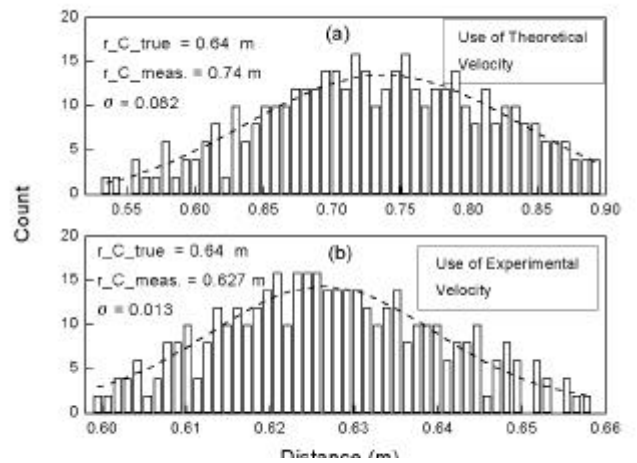


Fig. 8 Histogram of the estimated distance r_C : (a) theory, (b) experiments